

Evidence of local effects in anomalous refraction and focusing properties of dodecagonal photonic quasicrystals

Emiliano Di Gennaro,^{1,*} Carlo Miletto,¹ Salvatore Savo,¹ Antonello Andreone,¹ Davide Morello,² Vincenzo Galdi,² Giuseppe Castaldi,² and Vincenzo Pierro²

¹CNISM and Department of Physics, University of Naples “Federico II,” Piazzale Tecchio 80, I-80125 Naples, Italy

²Waves Group, Department of Engineering, University of Sannio, Corso Garibaldi 107, I-82100 Benevento, Italy

(Received 10 April 2008; published 6 May 2008)

We present the key results from a comprehensive study of the refraction and focusing properties of a two-dimensional dodecagonal photonic “quasicrystal” (PQC), which was carried out via both full-wave numerical simulations and microwave measurements on a slab made of alumina rods inserted in a parallel-plate waveguide. We observe an anomalous refraction and focusing in several frequency regions, which confirm some recently published results. However, our interpretation, which is based on numerical and experimental evidence, substantially differs from the one in terms of “effective negative refractive index” that was originally proposed. Instead, our study highlights the critical role played by short-range interactions associated with local order and symmetry.

DOI: [10.1103/PhysRevB.77.193104](https://doi.org/10.1103/PhysRevB.77.193104)

PACS number(s): 42.70.Qs, 41.20.Jb, 42.30.-d, 61.44.Br

Since the pioneering work by Yablonovitch¹ and John,² “photonic crystals” (PCs) have elicited great attention from the scientific community, in view of the variety of peculiar electromagnetic (EM) band gap, waveguiding and/or confinement, refraction, and emission effects attainable through their use. Among the most intriguing applications, it is worth mentioning those related to negative refraction and subwavelength imaging (“superlensing”).^{3–6} The most typical PC configurations are based on dielectric inclusions (or voids) arranged according to *periodic* lattices in a host medium and can thus be studied by using well-established tools and concepts such as the Bloch theorem, unit cell, Brillouin zone, and equifrequency surfaces.

With specific reference to lensing applications, two different approaches have been presented to obtain a subwavelength resolution by using a dielectric PC slab. In the first one, a PC with a high dielectric contrast is tuned so as to behave (usually near a frequency band edge) like a homogeneous material with a negative refractive index $n=-1$,³ and the focus position of the flat lens follows a simple ray-optical construction.⁷ In the second approach, an “all angle negative refraction” (AANR) is achieved without an effective negative index, provided that the equifrequency surfaces (EFSs) of the PC are all convex and larger than the one pertaining to the host medium.⁸ In this case, the focus position does not follow the ray-optical construction and is *restricted*.⁹

During the last decade, the discovery in solid-state physics of certain metallic alloys (the so-called quasicrystals^{10,11}) whose X-ray diffraction spectra exhibit “noncrystallographic” rotational symmetries [e.g., fivefold or ($K > 6$)-fold, which are known to be incompatible with spatial periodicity] has generated a growing interest toward *aperiodically ordered* geometries, leading to the study of the so-called photonic quasicrystals (PQCs). In this framework, useful tools for geometrical parameterization can be borrowed from the theory of “aperiodic tilings.”¹² Several recent numerical and experimental studies have explored the EM properties of PQCs, in the form of two-dimensional (2D) aperiodic arrays of cylindrical rods or holes, as well as three-dimensional structures fabricated via stereolithography (see Ref. 13 and the references therein for a recent review of the subject).

The study of PQCs entails significant complications, from both theoretical and computational viewpoints, as compared to the study of standard (periodic) PCs. In spite of the lack of the aforementioned Bloch-type concepts and tools, approaches to the calculation of the density of states in PCQs have been proposed, relying, e.g., on rational approximants^{14,15} or on extended zone schemes in the reciprocal space.¹⁶ However, many PQC properties and underlying mechanisms, which generally involve short- and long-range interactions as well as complex multiple scattering phenomena, are not yet fully understood. Nevertheless, results have revealed the possibility of obtaining similar properties as those exhibited by periodic PCs, with interesting potentials (e.g., a richer band gap structure with lower and/or multiple frequencies of operation, higher isotropy, easier achievement of phase-matching conditions, etc.) in view of the additional degrees of freedom typically available in aperiodically-ordered structures.

Recently, some examples of 2D PQCs characterized by high-order (eightfold, 10-fold, and 12-fold) rotational symmetries have been proposed as good candidates to exhibit negative refraction and subwavelength focusing effects with polarization-insensitive and non-near-field imaging capabilities.^{17,18} Similar results were also obtained in the case of acoustic waves.¹⁹ Such effects and properties were interpreted in Ref. 17 within the framework of “effective negative refractive index and evanescent wave amplification.”

In this Brief Report, we present the key results from a comprehensive study, based on full-wave numerical simulations backed by experimental verifications, which show that the effective negative refractive index interpretation is questionable and unable to fully explain and predict the above effects, which instead arise from complex near-field scattering effects and short-range interactions critically associated to local symmetry points in the PQC.

The PQC of interest is a conformally scaled version of that in Ref. 17, made of dielectric alumina rods (relative permittivity $\epsilon_r=8.6$) of radius $r=0.4$ cm placed (in air) at the vertices of a square-triangle 12-fold-symmetric tiling with a lattice constant (tile side length) $a=1.33$ cm, and generated according to the Stampfli recursive construction²⁰ [see also

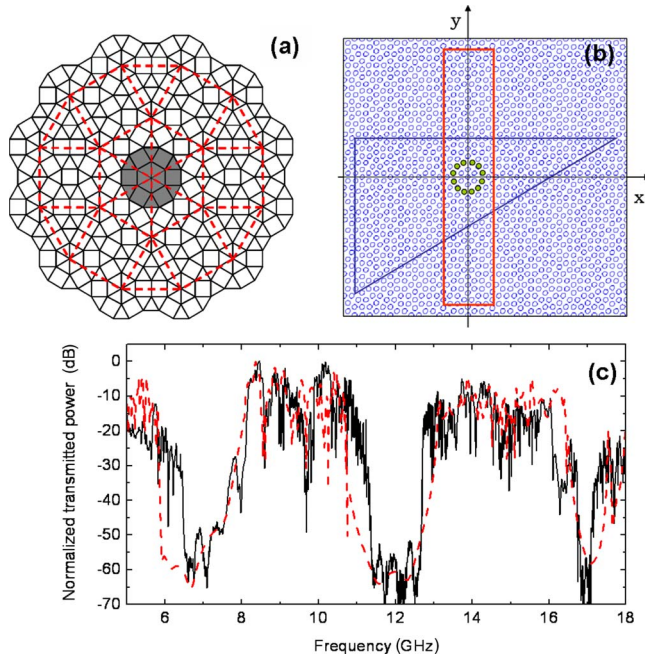


FIG. 1. (Color online) (a) Illustration of the Stampfli inflation rule. Starting from the parent tiling represented by the gray-shaded central dodecagon, a big parent (red/gray dashed lines) is generated by inflation, and filled up with copies of the original dodecagon placed at its vertices. (b) A portion of the tiling with the slab ($\sim 7a$ thickness) and wedge realizations considered in Ref. 17 (as well as in our study) marked by the red/gray and blue solid contours, respectively. The green/light gray-full-dot dodecagon corresponds to the parent tiling shown in (a). (c) Comparison (in a normalized scale) between the measured (black continuous curve) and simulated (red/gray dashed curve) transmitted power for the PQC slab in (b) with $a=1.33$ cm.

Fig. 1(a)]. Figure 1(b) illustrates two particular slab- and wedge-shaped tiling cuts (as in Ref. 17) considered in our study.

In our numerical simulations, assuming that the rods are infinitely long and parallel to the electric field, we employ a well-established full-wave technique (based on the Bessel-Fourier multipolar expansion²¹), which has been extensively applied to the study of 2D finite-size PCs²² and PQCs.²³ The experimental verification relies on microwave (X -band) measurements on PCQ slabs made of alumina rods of height $h=1$ cm inserted in an aluminum parallel-plate waveguide terminated with microwave absorbers, with a monopole antenna used to generate an electric field parallel to the rods. The intensity/phase maps are collected by using an HP8720C vector network analyzer and a computer-controlled x - y movable monopole antenna probe, in a setup similar to that described in Refs. 5 and 24.

As a preliminary check, we studied the transmission properties of the PQC slab in Fig. 1(b), for a fixed source position, within the 5–8 GHz frequency range. Figure 1(c) compares the experimental and simulated (normalized) transmitted power through the slab. Three main band gap regions are clearly observed, with fairly good agreement between simulations and measurements. We then studied the focusing properties within the frequency region 8–10 GHz

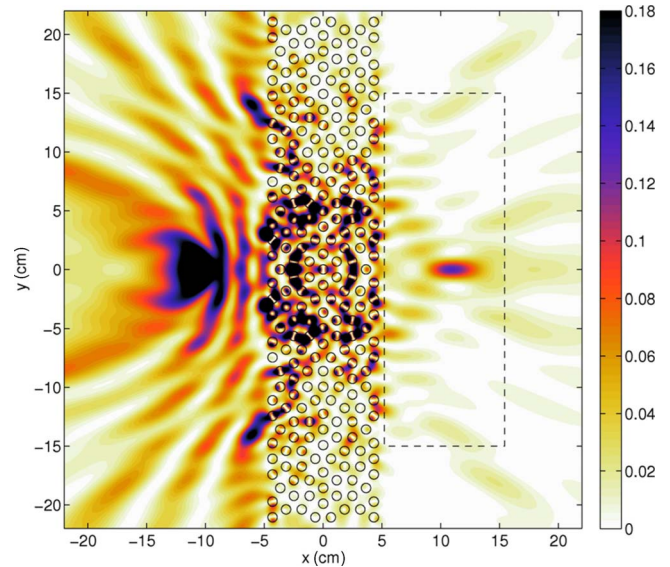


FIG. 2. (Color online) Simulated field intensity map at 8.836 GHz for a PQC slab as in Fig. 1(c) (with lateral a width of 42.9 cm and a thickness of 9.4 cm), illustrating the focusing of a source placed at $y_s=0$ and at a distance $d_x=6$ cm from the slab surface. The dashed rectangle delimits the 10×30 cm² area scanned in the image-side measurements.

(between the first and second band gaps) by observing the field intensity maps at the image side. We found several frequency regions (including those reported in Ref. 17) where a clear focus was visible, with the bandwidth ranging from a few megahertz to thousands of megahertz. We note that this feature represents a first remarkable difference with the (periodic) PC case, wherein the focusing regions tend to be more rare and well separated. The seemingly *denser* occurrence of focusing effects in PQCs could be attributed to their inherent self-similar nature.²⁵ We observed the most stable focusing effects around 8.350 GHz. However, in what follows, we concentrate on the focusing effects at 8.836 GHz, corresponding to the configuration considered in Ref. 17. In our study, the emphasis is not placed on *quantitative* assessments of the subwavelength focusing capabilities but rather on the phenomenology interpretation and its similarities and differences with respect to the periodic PC case.

Figure 2 shows an example of a field intensity map inside and outside the PQC slab in Fig. 1(b). It is worth noticing that such a slab is centered at the center of the tiling [$x=y=0$; see Fig. 1(b)], which is not only a center of local (12-fold) rotational symmetry but also possesses reflection symmetries with respect to both the x and the y axes. The presence of a focus at the image side is clearly observed. However, from a comprehensive numerical parametric study (see also Ref. 26 for more details), we found that neither a ray diagram approach can be used nor a preferential propagation direction can be established to justify and predict the image formation. Conversely, we found that a local structure [in particular, the green/light gray-full-dot dodecagon parent tiling highlighted in Fig. 1(b)] around the local symmetry center plays a key role.

If the PQC slab behaved like a homogeneous material with a negative refractive index $n=-1$, the source-image dis-

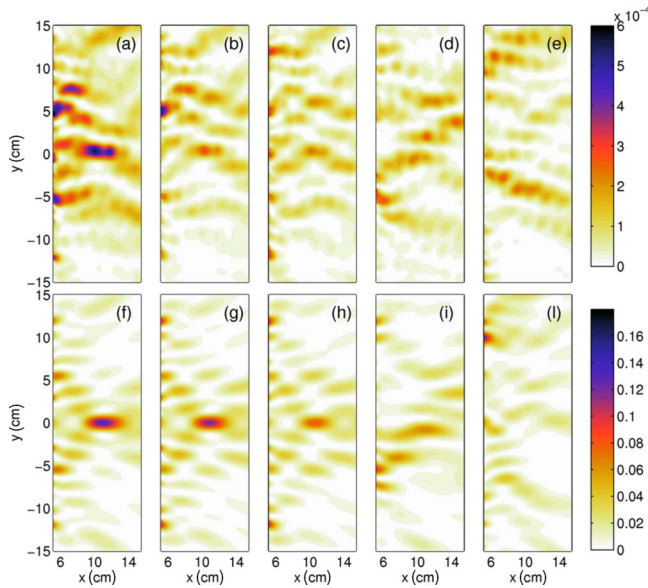


FIG. 3. (Color online) Same as in Fig. 2, but details of the measured [(a)–(e)] and simulated [(f)–(l)] field intensity maps at the image side for various source positions. [(a) and (f)] Source at $y_s=0$ and at a distance $d_x=6$ cm from the slab surface (cf. Fig. 2); [(b) and (g)] $y_s=0$ and $d_x=7$ cm; [(c) and (h)] $y_s=0$ and $d_x=8$ cm; [(d) and (i)] $y_s=1$ cm and $d_x=6$ cm; [(e) and (l)] $y_s=5$ cm and $d_x=6$ cm.

tance would remain constant and equal to twice the slab thickness.⁷ Results for periodic PCs showing an almost isotropic refractive response (see, e.g., Ref. 9) agree fairly well with this prediction. Moreover, in PC lenses, for lateral displacements of the source that preserve the distance from the lens interface as well as the structure periodicity, the focus remains unaffected, and its position follows the source location, in view of the absence of an optical axis. Figure 3 shows some representative measured and simulated field intensity maps at the image side of the PQC slab, for orthogonal and parallel (to the slab interface) displacements of the source. Again, general good agreement is observed between the simulations and the measurements. Specifically, Figs. 3(a) and 3(f) pertain to the configuration in Fig. 2, whereas Figs. 3(b), 3(c), 3(g), and 3(h) pertain to source displacements along the x -axis (i.e., orthogonal to the slab interface), which preserve the $y_s=0$ position (i.e., keeping the source facing the local symmetry center of the tiling). The focus position does not substantially change, raising further concerns about the interpretation in Ref. 17. Moving the source parallel to the slab surface, and therefore breaking the symmetry around the x -axis, one observes from Figs. 3(d), 3(e), 3(i), and 3(l) that even small displacements significantly affect the focus image, which undergoes a rapid deterioration until it completely disappears for the source placed at $y_s=5$ cm. Interestingly, a focus can be still observed as long as one extends the slab size along the y -axis and places the source at $y_s=13.67$ cm, i.e., directly facing the symmetry center of another big parent tiling [see Fig. 1(b)]. In this case, however, the image (not shown for brevity) exhibits a worse quality. The complex interplay between local and global order and symmetry in the focusing properties, which can be glanced from the above results, is confirmed by parametric

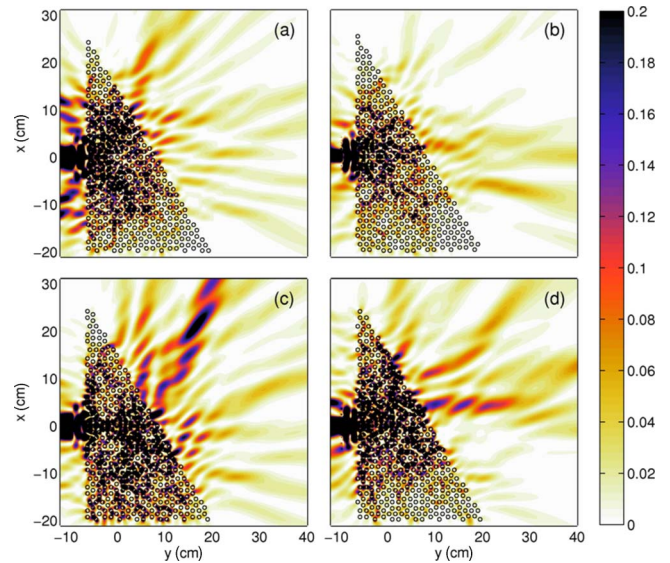


FIG. 4. (Color online) Simulated intensity field maps at 8.836 GHz for a collimated Gaussian beam (with minimum spot size of ~ 2.8 cm) normally impinging on several realizations of a PQC 60°-wedge. (a) Incident beam axis intersecting the local symmetry center, as in Ref. 17 and Fig. 2. [(b)–(d)] Different wedge realizations obtained by random rigid translations of the tiling (so as to displace the local symmetry center from the incident beam axis).

studies of PQC slabs of different thicknesses, wherein a variety of effects can be observed, which range from localized (single and multiple) spots to beaming phenomena (see Ref. 26 for details).

As a further check, we also carried out a numerical study that involved a collimated Gaussian beam impinging with normal incidence on the surface of PQC 60°-wedges extracted from the dodecagonal tiling. The results are shown in Fig. 4. Specifically, Fig. 4(a) pertains to the wedge realization shown in Fig. 1(b), with the incident beam axis intersecting the local symmetry center. Again, our results are similar to those in Ref. 17, with the transmitted beam propagating mainly in the “negative” direction—a phenomenon previously interpreted within the framework of an effective negative refractive index. However, a deeper study reveals that this effect too is critically related to the mutual position of the incident beam and the local symmetry center. This is clearly visible in Figs. 4(b)–4(d), which pertain to different PQC wedge samples obtained by random rigid translations of the tiling (so as to displace the local symmetry center from the incident beam axis), which display complex multibeam features in the transmitted field, thereby highlighting the absence of a clear-cut refractive behavior.

From the above results, which confirm the key role played by *short range* interactions involving a neighborhood of the parent tiling, one could speculate that the focusing properties of a PQC slab would be restricted to a limited range of incidence angles and should therefore occur also for significantly reduced lateral widths. Indeed, the focusing effects turn out to be rather *robust* with respect to lateral width reductions that do not significantly affect the modal field distribution in a neighboring region of the local symmetry center. Figure 5 shows the simulated and experimental results pertaining to a

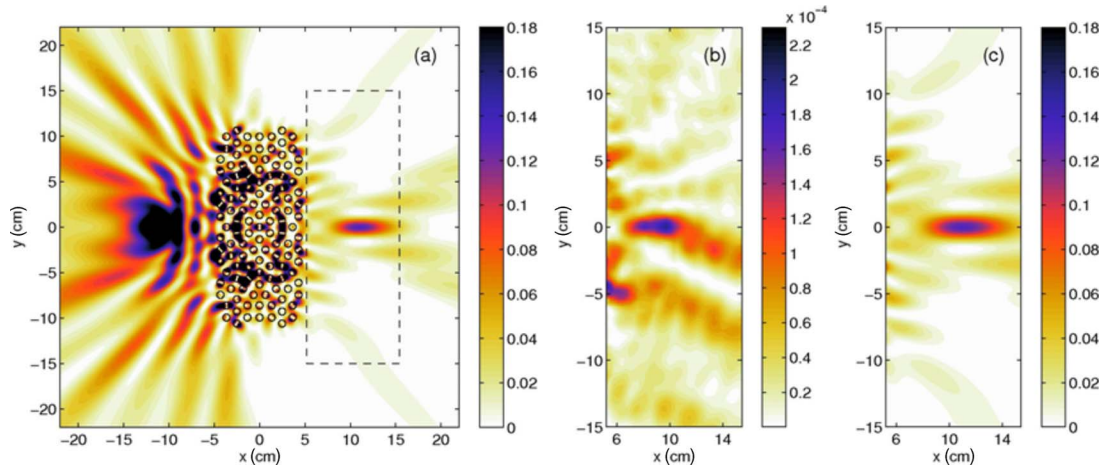


FIG. 5. (Color online) (a) Same as in Fig. 2, but for a PQC slab with lateral width reduced to 22 cm. [(b) and (c)] Details of the measured and simulated field intensity maps, respectively, at the image side.

PQC slab with a lateral width of only 22 cm (i.e., \sim six wavelengths, nearly one-half of that in Fig. 2) and yet still exhibiting a clear focus. Similar results were also obtained for PQC slabs with an even smaller (only three wavelengths) lateral width but with a larger thickness.²⁶

In conclusion, our numerical and experimental study of the refraction and focusing properties of dodecagonal PQCs confirms some of the results reported in the recent literature,¹⁷ but shows that, contrary to the original interpretation, such results are not attributable to an effective negative refractive index. Instead, they arise from complex near-field scattering effects and short-range interactions critically associated with local symmetry points in the PQC, which were only glossed over in previous studies. In this connec-

tion, it is worth recalling that local order and symmetry have already been observed to play a key role in a variety of PQC-related effects, including band gap formation,²³ field localization,²⁷ and directive emission.²⁸ The evidence and insights presented in this Brief Report constitute a further step toward a full understanding of the underlying mechanisms, which remains crucial for their judicious exploitation in the design of *compact* optical systems. Within this framework, further numerical and experimental studies of various PQC geometries are worth pursuing.

This work was funded by the Italian Ministry of Education and Scientific Research (MIUR) under the PRIN-2006 grant on “Study and realization of metamaterials for electronics and TLC applications.”

*emiliano@na.infn.it

¹E. Yablonovitch, Phys. Rev. Lett. **58**, 2059 (1987).

²S. John, Phys. Rev. Lett. **58**, 2486 (1987).

³M. Notomi, Phys. Rev. B **62**, 10696 (2000).

⁴S. Foteinopoulou and C. M. Soukoulis, Phys. Rev. B **72**, 165112 (2005).

⁵P. V. Parimi, W. T. Lu, P. Vodo, and S. Sridhar, Nature (London) **426**, 404 (2003).

⁶E. Cubukcu, K. Aydin, E. Ozbay, S. Foteinopoulou, and C. M. Soukoulis, Nature (London) **423**, 604 (2003).

⁷W. T. Lu and S. Sridhar, Opt. Express **13**, 10673 (2005).

⁸C. Luo, S. G. Johnson, J. D. Joannopoulos, and J. B. Pendry, Phys. Rev. B **68**, 045115 (2003).

⁹Y. Wang, X. Hu, X. Xu, B. Cheng, and D. Zhang, Phys. Rev. B **68**, 165106 (2003).

¹⁰D. Shechtman, I. Blech, D. Gratias, and J. W. Cahn, Phys. Rev. Lett. **53**, 1951 (1984).

¹¹D. Levine and P. J. Steinhardt, Phys. Rev. Lett. **53**, 2477 (1984).

¹²M. Senechal, *Quasicrystals and Geometry* (Cambridge University Press, Cambridge, UK, 1995).

¹³W. Steurer and D. Sutter-Widmer, J. Phys. D **40**, R229 (2007).

¹⁴A. E. Carlsson, Phys. Rev. B **47**, 2515 (1993).

¹⁵S. David, A. Chelnikov, and J. M. Lourtioz, IEEE J. Quantum Electron. **37**, 1427 (2001).

¹⁶M. A. Kaliteevski, S. Brand, R. A. Abram, T. F. Krauss, P.

Millar, and R. M. de la Rue, J. Phys.: Condens. Matter **13**, 10459 (2001).

¹⁷Z. Feng, X. Zhang, Y. Wang, Z. Y. Li, B. Cheng, and D. Z. Zhang, Phys. Rev. Lett. **94**, 247402 (2005).

¹⁸X. Zhang, Z. Li, B. Cheng, and D. Z. Zhang, Opt. Express **15**, 1292 (2007).

¹⁹X. Zhang, Phys. Rev. B **75**, 024209 (2007).

²⁰M. Oxborrow and C. L. Henley, Phys. Rev. B **48**, 6966 (1993).

²¹D. Felbacq, G. Tayeb, and D. Maystre, J. Opt. Soc. Am. A **11**, 2526 (1994).

²²A. A. Asatryan, K. Busch, R. C. McPhedran, L. C. Botten, C. M. de Sterke, and N. A. Nicorovici, Phys. Rev. E **63**, 046612 (2001).

²³A. Della Villa, S. Enoch, G. Tayeb, V. Pierro, V. Galdi, and F. Capolino, Phys. Rev. Lett. **94**, 183903 (2005).

²⁴P. V. Parimi, W. T. Lu, P. Vodo, J. Sokoloff, J. S. Derov, and S. Sridhar, Phys. Rev. Lett. **92**, 127401 (2004).

²⁵M. A. Kaliteevski, S. Brand, R. A. Abram, T. F. Krauss, R. M. de la Rue, and P. Millar, J. Mod. Opt. **47**, 1771 (2000).

²⁶E. Di Gennaro, D. Morello, C. Miletto, S. Savo, A. Andreone, G. Castaldi, V. Galdi, and V. Pierro, Photonics Nanostruct. Fundam. Appl. **6**, 60 (2008).

²⁷A. Della Villa, S. Enoch, G. Tayeb, F. Capolino, V. Pierro, and V. Galdi, Opt. Express **14**, 10021 (2006).

²⁸A. Micco, A. Della Villa, V. Galdi, F. Capolino, V. Pierro, S. Enoch, and G. Tayeb, arXiv:0711.3097 (unpublished).